Letter

Multigenerational memory in bacterial size control

Motasem ElGamel, Harsh Vashistha,* Hanna Salman, and Andrew Mugler†
Department of Physics and Astronomy, University of Pittsburgh, Pittsburgh, Pennsylvania, 15260, USA

(Received 13 June 2022; accepted 25 July 2023; published 12 September 2023)

Cells maintain a stable size as they grow and divide. Inspired by the available experimental data, most proposed models for size homeostasis assume size-control mechanisms that act on a timescale of one generation. Such mechanisms lead to short-lived autocorrelations in size fluctuations that decay within less than two generations. However, recent evidence from comparing sister lineages suggests that correlations in size fluctuations can persist for many generations. Here we develop a minimal model that explains these seemingly contradictory results. Our model proposes that different environments result in different control parameters, leading to distinct inheritance patterns. Multigenerational memory is revealed in constant environments but obscured when averaging over many different environments. Inferring the parameters of our model from *Escherichia coli* size data in microfluidic experiments, we recapitulate the observed statistics. Our paper elucidates the impact of the environment on cell homeostasis and growth and division dynamics.

DOI: 10.1103/PhysRevE.108.L032401

Cell size is a dynamic property of cells important for optimizing nutrient intake [1,2], accommodating intracellular content [2,3], and maintaining uniformity in tissues [4]. Cell size fluctuations are significant, yet constrained [5], suggesting active mechanisms of size control that go beyond initiating division a certain amount of time after birth [6–9]. Experiments and theory in recent years have revealed different phenomenological classes of size control [6,10–13]; connections between control of size, growth, and DNA replication [6,14–18]; and a surprising degree of heterogeneity in control mechanisms across, and even within, species [7,12,19]. Despite tremendous progress, basic questions remain open. In particular, it is still unclear whether deviations from the average size dissipate over one or many generations, and why the measured control parameters appear to vary so widely, even within lineages of the same population [12].

Most experiments suggest that deviations from the average cell size last for only a generation or so. Specifically, microfluidic experiments with bacteria using devices such as the "mother machine" [5] generally find an exponentially decaying autocorrelation function (ACF) in cell birth size $A_n = e^{-n/n_A}$ with $n_A \approx 1$ generation [10,12,16,19]. Recently, however, experiments that track two lineages born from the same mother cell (a "sisters machine") [20] have found something different. Measuring the Pearson cross-correlation function (PCF) between birth sizes in these experiments has also revealed an exponential decay, $P_n = e^{-n/n_P}$, but with $n_P \approx 3.5$ generations [Fig. 1(a), green]. Surprisingly, these same experiments show $n_A \approx 1$ generation for the lineages' ACF [Fig. 1(a), black], consistent with the mother machine experiments (see Supplemental Material [21] for details of how correlation functions are calculated in theory and experiments). This raises the question of whether size deviations last for only a generation, as implied by n_A, or for multiple generations, as implied by n_P. More generally, it raises the question of how a signal is transiently more correlated with another signal than with itself.

It is expected that size deviations dissipate within a generation in the context of adder size control [7,9,11,16,22,23]. Adder control means that a cell adds a constant amount to its birth size before dividing. To see the connection between adder control and how long size deviations last, consider a cell born with size x_n that grows exponentially for an elapsed phase ϕ_n, the product of the growth rate and cell cycle time [Fig. 1(b)]. After division, the daughter with fraction f_n will have birth size $x_{n+1} = f_n x_n e^{\phi_n}$. Defining $\epsilon_n = \ln(x_n/x_*)$ as the logarithmic deviation of the cell's birth size from the population-averaged birth size x_*, this expression becomes

$$\epsilon_{n+1} = \epsilon_n + \delta_n + \eta_n, \tag{1}$$

where $\delta_n = \phi_n - \ln 2$ and $\eta_n = \ln(2f_n)$ are deviations of the phase and fraction from their expected values for size doubling. Experiments in *Escherichia coli* have shown that η_n is Gaussian and uncorrelated between generations [24]. In this case, size control implies that the phase corrects for deviations in the birth size [10,12,19,22,25],

$$\delta_n = -\beta\epsilon_n + \xi_n, \tag{2}$$

where the homeostasis parameter β sets the strength of the correction, and ξ_n is uncorrelated Gaussian noise in the correction process. The values $\beta = 0$, $1/2$, and 1 correspond to the timer, adder, and sizer rules, respectively [6,12]. Experiments in bacteria generally observe a range of β values, centered around $1/2$ corresponding to the adder rule [7,12,19,26].

Combining Eqs. (1) and (2) gives a process $\epsilon_{n+1} = (1-\beta)\epsilon_n + \eta_n + \xi_n$ whose ACF $A_n = (1-\beta)^n$ and PCF $P_n = (1-\beta)^{2n}$ are straightforward to calculate [21]. For $\beta = 1/2$, we thus have $n_A = -1/\ln(1-\beta) \approx 1.4$ generations and

*Present address: Department of Molecular, Cellular and Developmental Biology, Yale University, New Haven, Connecticut 06511, USA.
†andrew.mugler@pitt.edu

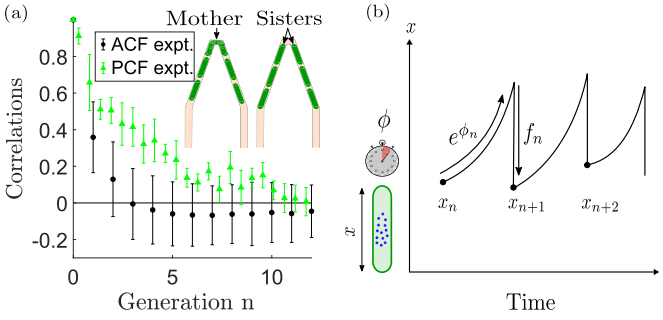

FIG. 1. (a) In the sisters machine (inset), a mother cell initiates two sister lineages in a common V-shaped channel [20]. Experiments [20] show that the autocorrelation function (ACF, black) for the cell birth size decays more quickly than the Pearson cross-correlation function between sister lineages (PCF, green). Here $n = 0$ is the shared mother cell. (b) A cell grows exponentially from an initial birth size x_n to a final division size $x_n e^{\phi_n}$, then divides by a fraction f_n.

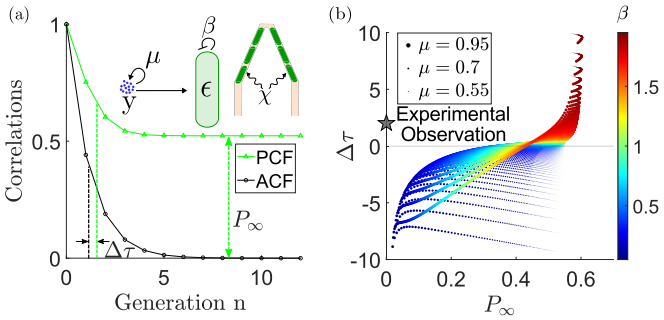

FIG. 2. The presence of common environmental fluctuations cannot explain the short-lived ACF and long-lived PCF observed in experiments [Fig. 1(a)]. (a) A long-lived protein y regulates cell size in two lineages subject to fast environmental noise χ (inset). The PCF [Eq. (5)] decays more slowly than the ACF [Eq. (4)] but has a large asymptote P_∞. (b) No parameters can explain the experimental timescale difference and zero asymptote. $\beta = 0.6$ and $\mu = 0.3$ in (a); $\sigma_\eta^2 = 0.0225$, $\sigma_\zeta^2 = 0.01$ and $\sigma_\chi^2 = 0.04$ in (a) and (b).

$n_P = n_A/2 \approx 0.7$ generations. While we see that n_A is about one generation for adder control, this framework cannot explain why n_P is observed in experiments to be multiple generations. Indeed, it is not clear from this framework how n_P could be larger than, not smaller than, n_A. Instead, we see that two noisy signals decorrelate twice as quickly from each other as each does from itself.

Here we resolve this disagreement between theory and experiment by going beyond the standard model of cell size control in Eqs. (1) and (2). Our fundamental premise is that the environment plays a defining role in setting the size control parameters, and that different channels within a microfluidic device are subject to different environments [27,28]. Because obtaining correlation functions from data often requires averaging over many channels to obtain sufficient statistics [12,19,20], we hypothesize that the averaging process obscures long timescales in some correlation functions (A_n) but not others (P_n). Inferring the parameters of our model from single-lineage autocorrelation data in *E. coli*, we find that this is indeed the case, suggesting that size correlations are multigenerational but dynamically diverse across environments. Our results suggest that size autocorrelations are compatible with an adder rule on average, but reveal the strong influence of a heterogeneous environment on individual lineages.

Before describing our main model, we first rule out the possibility that short autocorrelations and long cross-correlations between two lineages can be explained by the presence of common environmental fluctuations [29]. In principle, a signal with long intrinsic memory would exhibit short autocorrelations if this memory were overpowered by short-lived environmental noise. If this noise were common to both signals, the long memory would be expected to survive in the signal difference and therefore in the cross-correlation function. To investigate this possibility, we replace the noise term ξ_n in Eq. (2) with a long-lived, lineage-intrinsic component $y_n^{(i)}$ and a short-lived, environmental component χ_n,

$$\delta_n^{(i)} = -\beta\epsilon_n^{(i)} + y_n^{(i)} + \chi_n, \tag{3}$$

where $i = \{1, 2\}$ denotes each of the two sister lineages. Note that the intrinsic component $y_n^{(i)}$ depends on the lineage i, whereas the environmental component χ_n does not. By giving the intrinsic component, the dynamics $y_{n+1}^{(i)} = \mu y_n^{(i)} + \zeta_n^{(i)}$ with uncorrelated Gaussian noise $\zeta_n^{(i)}$, we allow for long-lived memory that approaches $(1-\mu)^{-1}$ generations as μ approaches one. A natural interpretation of y is the fluctuations in cellular protein content that regulates a cell's growth and metabolism and is inherited from one generation to the next. The environmental component χ_n is uncorrelated Gaussian noise.

Eliminating $\delta_n^{(i)}$ from Eqs. (1) and (3) gives $\epsilon_{n+1}^{(i)} = (1-\beta)\epsilon_n^{(i)} + y_n^{(i)} + \eta_n^{(i)} + \chi_n$, a dynamics for size fluctuations ϵ that depends on ϵ itself and on y, as depicted in the inset of Fig. 2(a). We solve for the ACF and PCF of $\epsilon_n^{(i)}$ by explicit iteration [21]. Defining $b = 1-\beta$, we obtain

$$A_n \propto c_1 b^n + c_2 \mu^n, \tag{4}$$

$$P_n \propto c_0 + c_3 b^{2n} + c_4 \mu^{2n} + c_5 b^n \mu^n, \tag{5}$$

where $c_0 = \sigma_\chi^2/f$, $c_1 = (\sigma_\chi^2 + \sigma_\eta^2)/f - b\sigma_\zeta^2/fgh$, $c_2 = \mu\sigma_\zeta^2/ghk$, $c_3 = \sigma_\zeta^2/fg^2 + \sigma_\eta^2/f$, $c_4 = \sigma_\zeta^2/g^2k$, $c_5 = -2\sigma_\zeta^2/g^2h$, $f = 1-b^2$, $g = \mu - b$, $h = 1-\mu b$, and $k = 1-\mu^2$. Each σ_i^2 is the variance of the corresponding noise term, and the proportionality constants in Eqs. (4) and (5) are set by the normalization condition $A_0 = P_0 = 1$. Because Eqs. (4) and (5) are not single exponential decays, we define a characteristic timescale as [30] $\tau_C = \sum_{n=0}^{\infty}(C_n - C_\infty)/(C_0 - C_\infty)$ for $C \in \{A, P\}$. Neglecting the fraction noise σ_η^2 (experiments show that $\sigma_\eta \approx 10\%$ [12]), this gives

$$P_\infty = \frac{\rho}{\rho + \ell}, \tag{6}$$

$$\tau_A = \frac{1}{\beta} + \left(\frac{1}{1-\mu}\right)\left[\frac{\mu(1+b)}{1+\mu b+\rho}\right], \tag{7}$$

$$\tau_P = \frac{1}{1-b^2} + \frac{1}{1-\mu^2} + \frac{2b\mu}{1-b^2\mu^2}, \tag{8}$$

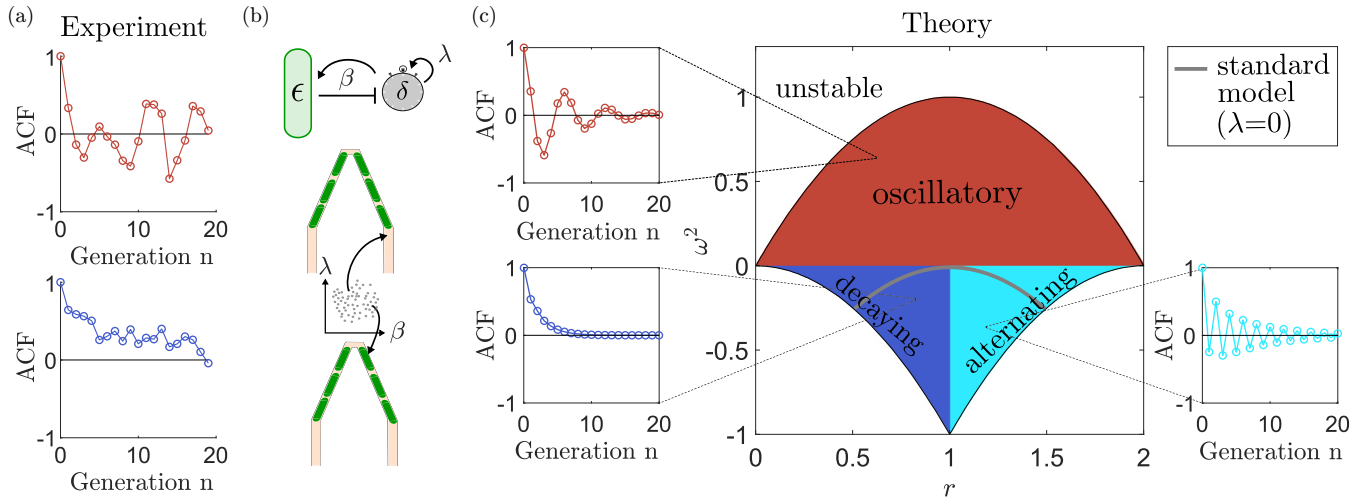

FIG. 3. Different dynamics in different environments. (a) Experimental birth size ACFs from single lineages in different channels [20] range from oscillatory to simple decay. (b) Our model includes size correction (β) and phase dependence (λ), with β and λ unique for each channel. (c) The model exhibits three stable dynamic regimes for the ACF, depending on the values of the damping rate $r = (1 + \beta - \lambda)/2$ and the squared underdamped frequency $\omega^2 = \beta - r^2$.

where $\rho = \sigma_\chi^2 hk/\sigma_\zeta^2$ and $\ell = (hk + fh - 2fk)/g^2$. We see that as μ approaches one, the second term in Eq. (8) dominates, and the PCF indeed becomes long-lived. However, for the ACF to remain short-lived ($\tau_A \sim 1/\beta$), we see that the second term in Eq. (7) must remain small, requiring $\rho \gg 1$. This condition increases the long-time cross-correlation P_∞, as seen in Eq. (6).

The requirement $\rho = \sigma_\chi^2 hk/\sigma_\zeta^2 \gg 1$ makes sense because, for short extrinsic noise to wash out long intrinsic memory, the noise must be strong ($\sigma_\chi^2 \gg \sigma_\zeta^2$). The fact that this then increases P_∞ also makes sense because strong extrinsic noise leaves two signals strongly correlated indefinitely. The net result is that the PCF timescale cannot be longer than the ACF timescale without a large PCF asymptote, as illustrated in Fig. 2(a). In fact, numerically probing all values of μ and β (with σ_η^2 nonzero), we find no value of $\Delta\tau = \tau_P - \tau_A$ and P_∞, consistent with the experimental observations of $\Delta\tau > 0$ and $P_\infty = 0$ [Fig. 2(b)]. We conclude that the observations in Fig. 1(a) cannot be explained by the presence of common environmental fluctuations.

If the environment is not providing strong fluctuations, is it playing an alternative role? To obtain insight into this question, we recognize that ACFs from individual lineages in different channels exhibit different dynamic behaviors, ranging from simple decay to oscillations [Fig. 3(a)] [12,19,20]. Oscillations in single-lineage ACFs could reflect insufficient data [16,19], although they persist even for lineages with hundreds of generations [12], suggesting that they may reflect genuine overcorrection in size control. We have checked using simulations that genuine oscillations are detectable for $N \geqslant 20$ generations (Fig. S1 [21]), and therefore we only analyze experimental lineages at least this long.

To explain the heterogeneity of dynamic behaviors, we hypothesize that the size-control parameters are a function of the environment, and that different channels have different environments. Environmental heterogeneity could be due to nutrient gradients on the length scale of the entire microfluidic device or mechanical differences among channels (mechanical forces limit growth in narrow channels, and actual channel widths can be different from designed widths [27]). Indeed, recent experimental analysis has shown that cells in different channels fluctuate around different homeostatic set points [24,28], consistent with the hypothesis of different environments.

To investigate this hypothesis, we modify Eq. (2) as

$$\delta_n^{(i)} = -\beta\epsilon_n^{(i)} + \lambda\delta_{n-1}^{(i)} + \xi_n^{(i)}, \tag{9}$$

where now $\xi_n^{(i)}$ is uncorrelated Gaussian noise. The new term in Eq. (9), $\lambda\delta_{n-1}^{(i)}$, introduces a dependence of the phase on its value in the previous generation. Physiologically, this dependence could result from the inheritance of fluctuations in key growth-control factors, such as ribosomes, RNA polymerases, and other proteins, from one generation to the next [24]. The dependence could be positive or negative, depending on whether the inherited factor primarily affects the growth rate or the cell cycle time [31]. Indeed, a similar term emerges naturally (along with β) from a systematic autoregression analysis of single-cell growth data [24], providing experimental evidence for the dependence [32]. In principle, λ could be perturbed by modulating the growth control factors, and β is known to increase for slower-growing cells [16,33].

As illustrated in Fig. 3(b) (top), Eqs. (1) and (9) contain feedback via (i) β, which compensates for a larger birth size via a smaller phase, and (ii) λ, which accounts for the generational dependence of the phase. Together, these terms produce damped, oscillatory dynamics, which can be seen by the following mapping: rearranging Eqs. (1) and (9) as $\epsilon_{n+1} - \epsilon_n = \delta_n + \eta_n$ and $\delta_{n+1} - \delta_n = -\beta\epsilon_n + (\lambda - \beta - 1)\delta_n + (\xi_{n+1} - \beta\eta_n)$, we can approximate their left-hand sides as time derivatives and combine them, yielding $\ddot{\epsilon} + 2r\dot{\epsilon} + (r^2 + \omega^2)\epsilon = \psi$, where $r = (1 + \beta - \lambda)/2$, $\omega^2 = \beta - r^2$, and $\psi_n = \xi_{n+1} + \eta_{n+1} - \lambda\eta_n$. These are the dynamics of a simple harmonic oscillator with damping rate r and underdamped frequency ω, driven by noise ψ.

Importantly, the parameters β and λ (and thus r and ω^2) are the same for each of the two lineages i in a channel

but vary from channel to channel [Fig. 3(b), bottom]. The question is whether different values of r and ω^2 can capture the dynamic heterogeneity observed in the experiments, and whether averaging over these values results in the observed auto- and cross-correlations.

To address this question, we solve for the ACF and PCF of $\epsilon_n^{(i)}$ in Eqs. (1) and (9) using the Z transform (the discrete-time analog of the Laplace transform) [21]. We obtain

$$A_n \propto q_- a_-^n + q_+ a_+^n, \tag{10}$$

$$P_n \propto s_- a_-^{2n} + s_+ a_+^{2n} - 2s a_-^n a_+^n, \tag{11}$$

where $a_\pm = 1 - r \pm \sqrt{-\omega^2}$; the coefficients $q_\pm$, $s_\pm$, and s are functions of $a_\pm$; and the noise strengths σ_η^2 and σ_ξ^2 [21], and again the proportionality constants, are set by $A_0 = P_0 = 1$. Stability requires $|a_\pm| < 1$, equivalent to the conditions $\omega^2 > -r^2$, $\omega^2 > -(r-2)^2$, and $\omega^2 < -r(r-2)$ [21] [bordering parabolas in Fig. 3(c)]. Damped oscillations occur when $\omega^2 > 0$ [horizontal line in Fig. 3(c)]. Alternation, which is unique to discrete systems when the ACF is dominated by a term with a factor of $(-1)^n$, occurs when $r > 1$ [21], [vertical line in Fig. 3(c)]. Together, these conditions give three dynamic regimes, illustrated in Fig. 3)c) [see Fig. S2(a) [21] for these regimes in the space of β and λ]. In particular, we see that simple decay (blue) and oscillations (red) are possible, as observed in the data. Oscillations are not possible in the standard model with $\lambda = 0$ [gray parabola in Fig. 3(c)].

Addressing whether our model explains the correlation data requires determining in which dynamic regimes the experiments lie. To this end, we estimate the parameters r and ω^2 in two ways. First, we perform a least-squares fit of Eq. (9) to each single-lineage dynamics, as a planar equation for $\delta_n^{(i)}$ versus $(\epsilon_n^{(i)}, \delta_{n-1}^{(i)})$; second, we fit Eq. (10) to each single-lineage ACF (see Ref. [21] for details). Consistent with our hypothesis [Fig. 3(b), bottom], in both cases we allow the r and ω^2 values to be different for different channels, but we require them to be the same for sister lineages in the same channel by combining the two sums of squares during fitting (relaxing this constraint results in a similar distribution of fitted values, Fig. S2(b) [21]). The resulting values of r and ω^2 for the two methods are shown in Fig. 4(a) (red and blue, respectively; see Fig. S2(a) [21] for these data in the space of β and λ). Values from data in a different growth condition also lie in the same parameter region (Fig. S2(b) [21]).

We see in Fig. 4(a) that the parameters inferred using either method generally lie in the decaying and oscillatory regimes (pink) but not the alternating regime (white). The parameters inferred from the ACF fits (blue) span a larger range than those inferred from the dynamics (red), but each case populates both regimes with various frequencies and damping strengths. Neither is confined to the standard model (gray parabola). Furthermore, the regime does not correlate with the length of the lineage [size of circle; see Fig. S2(b) for clarity], suggesting that observed dynamic features are not artifacts of insufficient data.

We therefore ask whether averaging over the decaying and oscillatory regimes [pink in Fig. 4(a)] is sufficient to explain the correlations observed in experiments. Performing this average, we obtain the results in Fig. 4(b) (pink). We see that the

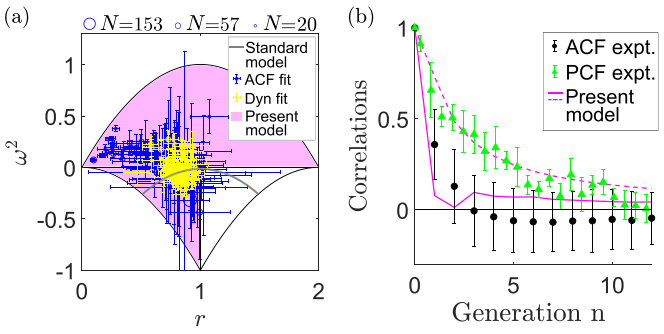

FIG. 4. Comparing theory and experiment. (a) r and ω^2 fitted from experimental single-lineage dynamics [red, Eq. (9)] or ACFs [blue, Eq. (10)]. Circle size: Lineage length N [top legend; see Fig. S2(b) for clarity]. (b) ACF [Eq. (10)] and PCF [Eq. (11)], averaged over r and ω^2 values from a (pink regions), compared with experimental results. $\sigma_\eta^2 = 0.09$ and $\sigma_\xi^2 = 0.04$ in (a) and (b).

averaged ACF is a relatively smooth function that decays in about a generation, consistent with the experimental averaged ACF [Fig. 4(b), black]. Evidently, oscillations with different frequencies are largely washed out in the averaging process [12,19], producing an apparent fast decay. We also see that the averaged PCF exhibits a longer timescale than the ACF, consistent with the experimental data [Fig. 4(b), green]. The reason is that an individual channel's PCF does not oscillate, even when the ACF does, because the PCF reports on the difference between two oscillatory signals, not the signals themselves. Consequently, the averaged PCF is sensitive to its longer-lived samples, whereas the averaged ACF appears short-lived due to the washout of many oscillation periods.

We have put forward a minimal model for cell size control that resolves the empirical paradox of short-lived autocorrelations but long-lived cross-correlations in cell size. We have found that cell-size memory is longer-lived than previously appreciated but is obscured in autocorrelations due to destructive interference among many oscillation periods. The results suggest that control parameters depend sensitively on the environment and that the environment varies considerably within a multichannel microfluidic device, as has been suggested [27] and demonstrated [24,28] previously.

The dynamics in Eq. (9) go beyond the standard model of cell size control ($\lambda = 0$) and have a structure motivated by recent single-cell growth experiments [24]. Parameters inferred from these dynamics [Fig. 4(a), red] occupy the same regimes but nevertheless a narrower range than parameters inferred from the ACFs [Fig. 4(a), blue], suggesting that the dynamics may be incomplete. A more accurate dynamical model might include nonlinear terms, relate more than two consecutive generations, or involve time-dependent parameters (we have checked in Fig. S3 [21] that temporal parameter fluctuations have little effect on the correlation functions). Equations (1) and (9) are not unique in generating Eqs. (10) and (11), and it will be interesting to see whether the dynamic control mechanism can be better pinpointed in future work.

Our central prediction that heterogeneous environments obscure multigenerational timescales in the averaged ACF could be tested by modulating the degree of heterogeneity in the channel environments. To the extent that the heterogeneity

is nutrient-limited, it could be modulated either by flowing nutrients overtop the cell traps, which would reduce heterogeneity, or by inducing chemical gradients along the device, which would increase heterogeneity. Both are feasible options for future experiments.

We thank Michael Vennettilli for introducing us to the Z transform. This work was supported by National Science Foundation Grants No. DMS-2245816 to A.M. and H.S., No. PHY-2118561 to A.M., and No. PHY-2014116 to H.S.

[1] A.-C. Chien, N. Hill, and P. Levin, Curr. Biol. **22**, R340 (2012).
[2] J. J. Turner, J. C. Ewald, and J. M. Skotheim, Curr. Biol. **22**, R350 (2012).
[3] W. F. Marshall, K. D. Young, M. Swaffer, E. Wood, P. Nurse, A. Kimura, J. Frankel, J. Wallingford, V. Walbot, X. Qu *et al.*, BMC Biol. **10**, 101 (2012).
[4] M. B. Ginzberg, R. Kafri, and M. Kirschner, Science **348**, 1245075 (2015).
[5] P. Wang, L. Robert, J. Pelletier, W. L. Dang, F. Taddei, A. Wright, and S. Jun, Curr. Biol. **20**, 1099 (2010).
[6] A. Amir, Phys. Rev. Lett. **112**, 208102 (2014).
[7] L. Willis and K. C. Huang, Nat. Rev. Microbiol. **15**, 606 (2017).
[8] G. Facchetti, F. Chang, and M. Howard, Curr. Opin. Syst. Biol. **5**, 86 (2017).
[9] P.-Y. Ho, J. Lin, and A. Amir, Annu. Rev. Biophys. **47**, 251 (2018).
[10] S. Taheri-Araghi, S. Bradde, J. T. Sauls, N. S. Hill, P. A. Levin, J. Paulsson, M. Vergassola, and S. Jun, Curr. Biol. **25**, 385 (2015).
[11] I. Soifer, L. Robert, and A. Amir, Curr. Biol. **26**, 356 (2016).
[12] L. Susman, M. Kohram, H. Vashistha, J. T. Nechleba, H. Salman, and N. Brenner, Proc. Natl. Acad. Sci. USA **115**, E5679 (2018).
[13] G. Facchetti, B. Knapp, F. Chang, and M. Howard, Biophys. J. **117**, 1728 (2019).
[14] P.-Y. Ho and A. Amir, Front. Microbiol. **6**, 662 (2015).
[15] F. Barber, P.-Y. Ho, A. W. Murray, and A. Amir, Front. Cell Dev. Biol. **5**92 (2017).
[16] F. Si, G. Le Treut, J. T. Sauls, S. Vadia, P. A. Levin, and S. Jun, Curr. Biol. **29**, 1760 (2019).
[17] G. Witz, E. van Nimwegen, and T. Julou, Elife **8**, e48063 (2019).
[18] M. Berger and P. R. t. Wolde, Nat. Commun. **13**, 6556 (2022).
[19] Y. Tanouchi, A. Pai, H. Park, S. Huang, R. Stamatov, N. E. Buchler, and L. You, Nature (London) **523**, 357 (2015).
[20] H. Vashistha, M. Kohram, and H. Salman, eLife **10**, e64779 (2021).
[21] See Supplemental Material https://link.aps.org/supplemental/10.1103/PhysRevE.108.L032401 for additional derivations and data analysis.
[22] M. Campos, I. V. Surovtsev, S. Kato, A. Paintdakhi, B. Beltran, S. E. Ebmeier, and C. Jacobs-Wagner, Cell **159**, 1433 (2014).
[23] L. K. Harris and J. A. Theriot, Cell **165**, 1479 (2016).
[24] M. Kohram, H. Vashistha, S. Leibler, B. Xue, and H. Salman, Curr. Biol. **31**, 955 (2021).
[25] M. Osella, E. Nugent, and M. C. Lagomarsino, Proc. Natl. Acad. Sci. USA **111**, 3431 (2014).
[26] S. Jun, F. Si, R. Pugatch, and M. Scott, Rep. Prog. Phys. **81**, 056601 (2018).
[27] D. Yang, A. D. Jennings, E. Borrego, S. T. Retterer, and J. Männik, Front. Microbiol. **9**, 871 (2018).
[28] A. Stawsky, H. Vashistha, H. Salman, and N. Brenner, iScience **25**, 103678 (2022).
[29] M. B. Elowitz, A. J. Levine, E. D. Siggia, and P. S. Swain, Science **297**, 1183 (2002).
[30] S. Fancher and A. Mugler, Elife **9**, e58981 (2020).
[31] Inheritance of protein content could affect the growth rate and the cell cycle time in different ways. Inheritance of growth proteins (e.g., ribosomes) could result in positive λ [24]: a mother with more-than-average growth proteins will grow fast and produce a daughter with more-than-average growth proteins that also grows fast. Inheritance of division proteins (e.g., FtsZ) that may need to reach a fixed threshold at division could result in negative λ: a mother born with more-than-average division proteins will take less time to reach the threshold and divide, but if the threshold is met precisely, the daughter will then be born with a closer-to-average amount of division proteins, and thus take an average amount of time to divide. This will correct the mother's deviation in the cell cycle time, corresponding to a negative dependence.
[32] In Ref. [24], the phase variable depends on the growth rate, which depends on its value in the previous generation. In our model, the phase variable depends directly on its value in the previous generation. Both models fall in the same phenomenology class (capable of oscillations and decay), and because we seek the simplest member of this class, we choose the simpler model.
[33] M. Wallden, D. Fange, E. G. Lundius, Ö. Baltekin, and J. Elf, Cell **166**, 729 (2016).